JOURNAL OF GUIDANCE, CONTROL, AND DYNAMICS
Vol. 21, No. 2, March–April 1998

Natural Description of Aircraft Motion

Giulio Avanzini*
University of Rome "La Sapienza," Rome 00184, Italy
Guido de Matteis†
Turin Polytechnic Institute, Turin 10129, Italy
and
Luciano de Socio‡
University of Rome "La Sapienza," Rome 00184, Italy

Reference is made to the various approaches leading to the timescale separation in aircraft dynamics. A separation of the translational variables as slow states from the fast rotational ones is assumed as the starting point to show that the Frenet triad can be conveniently adopted to develop algebraic expressions for the trajectory dynamics of the aircraft. The solution of the aircraft motion is realized by first dividing the time domain into intervals, the duration of which is of the order of magnitude of the characteristic time of the slow dynamics. Then, slow states such as vehicle position and velocity are immediately obtained over the entire interval in the form of a series expansion. Finally, the equations of the fast subsystem are numerically integrated in the same interval. The accuracy and efficiency of the proposed procedure is discussed in comparison with the straight numerical integration of the full system of governing equations. The method lends itself to applications in trajectory optimization and inverse simulation problems.

Nomenclature

g	= acceleration of gravity
J_x, J_y, J_z, J_{xz}	= moments and product of inertia
k_1, k_2	= curvature and torsion
L, M, N	= aerodynamic moment components
$\boldsymbol{L}_{IB}, \boldsymbol{L}_{IF}$	= transformation matrices
m	= mass
p, q, r	= angular velocity components
$\boldsymbol{R}$	= inertial position
R_N, R_E, R_D	= inertial position coordinates: north, east, and down, respectively
s	= curvilinear abscissa
T	= thrust force modulus
t	= time
u, v, w	= velocity components in body axes
V	= velocity modulus
$\boldsymbol{V}$	= velocity vector
V_N, V_E, V_D	= inertial velocity components
X, Y, Z	= aerodynamic force components in body axes
$\boldsymbol{x}$	= state vector
x, y, z	= c.g. coordinates in the Frenet triad
α	= angle of attack
β	= sideslip angle
Δt_i	= time interval, s
$\Delta\eta_i$	= time step of numerical integration
$\delta_A, \delta_E, \delta_R$	= aileron, elevator, and rudder angles, respectively
δ_T	= throttle setting
δt	= step size for numerical differentiation
$\boldsymbol{\xi}$	= c.g. position vector in the Frenet triad
ρ	= air density
$\boldsymbol{\Phi}$	= Euler angle vector
ϕ, θ, ψ	= Euler angles
$\boldsymbol{\omega}$	= angular velocity

Subscripts

f	= fast timescale
s	= slow timescale
0	= initial value, either s equal to 0 or t equal to t_0

Presented as Paper 96-3375 at the AIAA Atmospheric Flight Mechanics Conference, San Diego, CA, July 29–31, 1996; received Aug. 27, 1996; revision received Aug. 18, 1997; accepted for publication Aug. 20, 1997.

*Ph.D. Student, Department of Mechanics and Aeronautics, via Eudossiana 18.
†Professor, Department of Aerospace Engineering, corso Duca degli Abruzzi 24. Member AIAA.
‡Professor, Department of Mechanics and Aeronautics, via Eudossiana 18. Member AIAA.

I. Introduction

IN this work a procedure is proposed for the direct simulation of aircraft dynamics. From considerations that the timescale separation (TSS) can be used to decouple the c.g. dynamics from the attitude dynamics, it is shown that the aircraft trajectory can be expressed by an algebraic form over a discrete time interval after reference is made to its natural coordinates.[1]

The need was felt for TSS in aircraft dynamics for reducing the computational cost in real-time simulations or for determining approximate solutions to the airplane dynamics as required in the evaluation of the stability characteristics in the design of the control system in the solution of inverse control problems. In general, the aim was to reduce the order and the degree of the fundamental set of equations that governs the airplane dynamics.

Systematic studies on TSS have been developed for about the last three decades. The problems in which the TSS is adopted can be divided into two main groups. The first group corresponds to problems related to the aircraft trajectory optimization and involves consideration of the c.g. dynamics only. In these cases, the main goal is to find analytic solutions to simplified forms of the governing equations, and the treatment is based on the theory of singular perturbations. The procedure then requires that some state variables be subjected to changes according to characteristic times, which are of order ϵ with respect to the characteristic times of some other variables. This leads to a power series expansion of the unknowns in terms of ϵ after such a parameter has been recognized. The mathematical foundations of the works in this field are sound, although in some cases, from the application point of view, the small parameter ϵ is of order one. In the existing literature, significant examples are those by Ardema[2] and by Calise and Markopoulos.[3] Both Refs. 2 and 3 deal with the search for analytic, optimal solutions to performance problems, and, in particular, Ref. 3 more deeply investigates the mathematical aspects and is more explicitly conscious of the many difficulties. The need for a systematic approach for identifying ϵ, via nondimensionalization of the state variables, is particularly stressed in Ref. 3, although such a nondimensionalization is not usually sufficient, and ad hoc assumptions still are often necessary.

The second group of problems deals with the design of flight control systems for nonlinear trajectories. Again, in related works[4–7] the singular perturbation theory is adopted, following a postulated existence of slow and fast (and, sometimes, intermediate) state variables. Then there is a formal separation of the c.g. motion equations from the equations for the attitude dynamics. The zeroth-order terms of the slow variables expansion and the first-order, nonzero fast variables appear, respectively, in the two sets of equations. The identification of the small parameter ϵ is not even attempted. However, the results of the procedure are very satisfactory in most cases, particularly when a significant difference in timescales between the fast and slow states is present,[6] as the technique allows one to obtain a very suitable reduction of the order of the dynamic system,[7] simplifies the linearizing transformations in the synthesis of trajectory controllers, and provides a consistent means for eliminating ignorable state variables.[4]

In all of the aforementioned cases, either those where the small ϵ of the matched asymptotic expansions could be really identified or those where the existence of such a small parameter was postulated, the reduction of the system order followed from the presence of a wide separation in dynamics among the state variables. In particular, in those cases where the full dynamics of the aircraft were dealt with,[4–7] the longer time was associated to the aircraft translational variables and the shorter time to the rotations about the c.g.

In this study, by keeping the assumptions on the TSS just discussed, the slow, c.g. dynamics is solved by an algebraic formulation, which applies over a time interval of the order of the long characteristic time. The formulation of this approach stands on the basic result, from differential geometry, that any curve in a three-dimensional space can be locally approximated by a helix provided that some conditions on its derivatives are satisfied.[1] Thus, the aircraft trajectory appears to be a natural candidate to be represented very closely by this helix. Leaving the details of the analysis to the following section, the c.g. location along the flight path is conveniently expressed by a power series expansion in terms of the curvilinear abscissa s, the coefficients of which are functions of the natural or intrinsic coordinates, i.e., the curvature k_1 and the torsion k_2, and their derivatives.

As a consequence, once the overall system dynamics are separated into slow and fast subsystems, the simulation of the aircraft motion can be realized by first dividing the entire time domain into intervals Δt_i, each interval corresponding to a tract of the c.g. path along which the error associated to the power series expansion of the current location is kept below an assigned value. The initial curvature and, in case a better approximation is desired, its s derivative and the torsion are easily evaluated from the dynamical state at the initial time of the interval. At this point, all of the characteristics of the c.g. motion are immediately known. Then, as a second step, the set of differential equations governing the fast attitude dynamics is numerically solved in each interval Δt_i.

The proposed procedure allows the direct simulation of the full dynamics of the aircraft with a reduction of computer time as compared with the numerical integration of the complete set of equations, inasmuch as a problem of lower order is solved. Furthermore, the expression in the new formulation of the trajectory variables can be very convenient in performance optimization and in the solution of inverse problems where a time-defined, three-dimensional trajectory is to be realized by the aircraft.[8]

The next section will present the details of the procedure for solution of the governing equations based on TSS. In Sec. III the adopted model of the F-16 fighter aircraft will be briefly recalled, and some significant maneuvers will be simulated to show the validity of the trajectory representation by a piecewise helix and to discuss the accuracy of the integration method.

II. Analysis

The dynamics of a rigid aircraft is governed by the following set of flat-Earth equations for zero ambient wind[9]:

$$\dot{\boldsymbol{V}} = \begin{bmatrix} \dot{V}_N \\ \dot{V}_E \\ \dot{V}_D \end{bmatrix} = \frac{\boldsymbol{L}_{IB}}{m} \begin{bmatrix} X+T \\ Y \\ Z \end{bmatrix} + \begin{bmatrix} 0 \\ 0 \\ g \end{bmatrix} \tag{1}$$

$$\dot{\boldsymbol{R}} = \begin{bmatrix} \dot{R}_N \\ \dot{R}_E \\ \dot{R}_D \end{bmatrix} = \boldsymbol{V} \tag{2}$$

$$\dot{\boldsymbol{\omega}} = \begin{bmatrix} (A_p J_z + A_r J_{xz}) \big/ \left(J_x J_z - J_{xz}^2\right) \\ \left[J_{xz}(r^2 - p^2) + (J_z - J_x) pr + M\right] \big/ J_y \\ (A_r J_x + A_p J_{xz}) \big/ \left(J_x J_z - J_{xz}^2\right) \end{bmatrix} \tag{3}$$

where $\boldsymbol{\omega} = (p, q, r)^T$ and

$$A_p = J_{xz} pq + (J_y - J_z) qr + L$$

$$A_r = -J_{xz} qr + (J_x - J_y) pq + N$$

Then

$$\dot{\boldsymbol{\Phi}} = \begin{bmatrix} 1 & \sin\phi\tan\theta & \cos\phi\tan\theta \\ 0 & \cos\phi & -\sin\phi \\ 0 & \sin\phi\sec\theta & \cos\phi\sec\theta \end{bmatrix} \begin{bmatrix} p \\ q \\ r \end{bmatrix} \tag{4}$$

where $\boldsymbol{\Phi} = (\phi, \theta, \psi)^T$. In the preceding set, $\boldsymbol{R}$ is the position vector of the aircraft c.g. in the inertial frame $\mathcal{F}_I$, with R_D directed vertically downward, and Eq. (1) is referred to $\mathcal{F}_I$, whereas Eq. (3) is referred to a body-fixed frame $\mathcal{F}_B$, with $\boldsymbol{L}_{IB}(-\phi, -\theta, -\psi)$ the transformation matrix from $\mathcal{F}_B$ to $\mathcal{F}_I$. Also, (X, Y, Z) and (L, M, N) are the aerodynamic force and moment components, respectively, which depend on the velocity modulus $V = |\boldsymbol{V}|$, the aerodynamic angles α and β, the rotational velocity $\boldsymbol{\omega}$, the density $\rho(R_D)$, and the control angles. Finally, Eq. (4) provides Euler angles rates as a function of the angular velocity components. Therefore, the state of the system, in general, is given by the vector $\boldsymbol{x} = (\boldsymbol{V}, \boldsymbol{R}, \boldsymbol{\omega}, \boldsymbol{\Phi})^T$ with 12 scalar components, and its evolution is formally expressed in state-space form as

$$\dot{\boldsymbol{x}} = \boldsymbol{f}(\boldsymbol{x}, \boldsymbol{u}), \qquad \boldsymbol{x}(t=0) = \boldsymbol{x}_0 \tag{5}$$

where $\boldsymbol{u}$ is the control vector.

As stated in the preceding section, the set of components of $\boldsymbol{x}$ can be divided into two subsets, the first one corresponding to the slowly changing states and the second one associated with the fast ones. In this context, the words *slow* and *fast* refer to variables that respond to the actions of the controls with slow and fast variations, respectively. Therefore,[7]

$$\boldsymbol{x} = (\boldsymbol{x}_s, \boldsymbol{x}_f)^T \tag{6}$$

where $\boldsymbol{x}_s = (\boldsymbol{V}, \boldsymbol{R})^T$ and $\boldsymbol{x}_f = (\boldsymbol{\omega}, \boldsymbol{\Phi})^T$.

Let us consider the trihedron of unit vectors $\hat{\boldsymbol{\tau}}$, $\hat{\boldsymbol{\nu}}$, and $\hat{\boldsymbol{b}}$ moving along the trajectory, where $\hat{\boldsymbol{\tau}}$ is along the tangent, and $\hat{\boldsymbol{\nu}}$ and $\hat{\boldsymbol{b}}$ are along the radius of curvature and the binormal, respectively. This system, shown in Fig. 1, is also called Frenet's triad $\mathcal{F}_F$. At a given time $t = t_0$, let us consider $\mathcal{F}_F$ with the origin O_F in the location of the aircraft c.g. The transformation matrix from $\mathcal{F}_F$ to $\mathcal{F}_I$ is

$$\boldsymbol{L}_{IF} = \left(\frac{\boldsymbol{V}}{V}, \frac{\boldsymbol{n}}{|\boldsymbol{n}|}, \frac{\tilde{\boldsymbol{V}}\boldsymbol{n}}{V|\boldsymbol{n}|} \right)_0 \tag{7}$$

where $\boldsymbol{n} = \dot{\boldsymbol{V}} - \boldsymbol{V}\dot{V}/V$, $\tilde{\boldsymbol{V}}\boldsymbol{n}$ is the matrix equivalent of the cross product, $\dot{\boldsymbol{V}}$ is given by Eq. (1), and the subscript 0 stays for $t = t_0$.

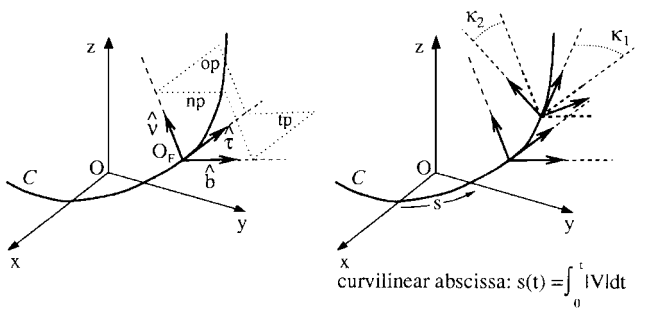

Fig. 1 Frenet triad and intrinsic coordinates: tp, tangent plane; op, osculating plane; np, normal plane; curvature, $k_1 = d\kappa_1/ds$; and torsion, $k_2 = d\kappa_2/ds$.

We then recall that any algebraic curve in three dimensions can be locally expressed in $\mathcal{F}_F$ by the series expansion[1]

$$\boldsymbol{\xi} = \begin{bmatrix} x(s) \\ y(s) \\ z(s) \end{bmatrix} = \begin{bmatrix} s - s^3\left(k_1^2\right)_0/3! \\ s^2(k_1)_0/2! + s^3(k_1')_0/3! \\ s^3(k_1k_2)_0/3! \end{bmatrix} + 0[s^4] \quad (8)$$

after reference has been made to the intrinsic or natural coordinates s, k_1, and k_2, namely, the curvilinear coordinate along the c.g. trajectory, the curvature, and the torsion, respectively. In particular, the curvature k_1 gives the rate of change of the normal plane about $\hat{\boldsymbol{b}}$, and the torsion k_2 represents the rate of change of the osculating plane about $\hat{\boldsymbol{\tau}}$. Again, the subscript 0 indicates $s = 0$ if $s(t = t_0) = 0$.

Because $\dot{s} = V$, and with reference to the c.g. trajectory, we can write

$$s(t) = V_0(t-t_0) + \tfrac{1}{2}\dot{V}_0(t-t_0)^2 + \tfrac{1}{3!}\ddot{V}_0(t-t_0)^3 + 0\left[(t-t_0)^4\right] \quad (9)$$

Using the relations (8) and their time derivatives to express $\dot{\boldsymbol{\xi}}$ and then projecting $\boldsymbol{\xi}$ and $\dot{\boldsymbol{\xi}}$ into the inertial frame $\mathcal{F}_I$, it is direct to obtain the slow dynamics variables over a time interval of the order of magnitude of the long characteristic time. In this respect, from the differential geometry, curvature and torsion can be expressed in the following forms[1]:

$$k_1 = (1/V^2)(|\dot{\boldsymbol{V}}|^2 - \ddot{s}^2)^{\frac{1}{2}} \quad (10)$$

$$k_2 = \frac{\det\{\boldsymbol{V}, \dot{\boldsymbol{V}}, \ddot{\boldsymbol{V}}\}}{V^2(|\dot{\boldsymbol{V}}|^2 - \ddot{s}^2)} \quad (11)$$

As a consequence, the expansion parameters $(k_1)_0$ and $(k_2)_0$ and the derivative $(k_1')_0 = (\mathrm{d}k_1/\mathrm{d}s)_0$ in Eqs. (8) are evaluated as functions of $\boldsymbol{V}_0, \dot{\boldsymbol{V}}_0$, and $\ddot{\boldsymbol{V}}_0$, which correspond to the initial state of the slow system.

Note that, if we limit the series expansion of $y(s)$, $z(s)$, and $s(t)$ [Eqs. (8) and (9)] to the quadratic terms, then the calculation of the current position s and of $\boldsymbol{\xi}$ is straightforward because only the state and control variables at $t = t_0$ are required for the evaluation of $(k_1)_0$ and $\dot{\boldsymbol{V}}_0$, and the remainders represent the errors of truncation. If we sum one more term in the series, the improvement in accuracy depends on the accuracy in computing $\ddot{\boldsymbol{V}}_0$, $(k_1')_0$, and $(k_2)_0$ numerically. In particular, for the approximation of $\dot{\boldsymbol{V}}$, this time derivative is determined by a centered finite difference algorithm, i.e., $\ddot{\boldsymbol{V}} = [\dot{\boldsymbol{V}}(t_0 + \delta t) - \dot{\boldsymbol{V}}(t_0 - \delta t)]/2\delta t$, where, by writing in concise form $\dot{\boldsymbol{V}} = \boldsymbol{h}(\boldsymbol{x}, \boldsymbol{u})$, it is $\dot{\boldsymbol{V}}(t_0 \pm \delta t) = \boldsymbol{h}[\boldsymbol{x}(t_0 \pm \delta t), \boldsymbol{u}(t_0 \pm \delta t)]$ with $\boldsymbol{x}(t_0 \pm \delta t) = \boldsymbol{x}(t_0) \pm \dot{\boldsymbol{x}}(t_0)\delta t$. The value of δt is selected to give the required accuracy.

In the solution of the aircraft motion, the integration domain is divided into a number of time intervals, the length Δt_i of which is related to the timescale of the slow dynamics. Thus, the variable η_i is defined as $t_{i-1} \le \eta_i \le t_i$. In the ith interval the velocity modulus is expanded as

$$V(\eta_i) = V(t_i) + \dot{V}(t_i)\eta_i + \frac{\ddot{V}(t_i)}{2}\eta_i^2 \quad (12)$$

We also define the vector $\Xi(\eta_i) = (\boldsymbol{\xi}, \dot{\boldsymbol{\xi}})^T$ so that the slow states are expressed as

$$\boldsymbol{x}_s(\eta_i) = \begin{bmatrix} \boldsymbol{L}_{IF}(t_i) & 0 \\ 0 & \boldsymbol{L}_{IF}(t_i) \end{bmatrix} \Xi(\eta_i) \quad (13)$$

Again, the components of $\Xi(\eta_i)$ can be obtained in a way that is either analytical or in part numerically calculated. In both cases, the order of magnitude of the truncation error provides the order of magnitude of Δt_i.

At this point the dynamics of the fast subsystem is governed by

$$\dot{\boldsymbol{x}}_f = \boldsymbol{g}(\boldsymbol{x}_f, \boldsymbol{u}, \boldsymbol{x}_s; \eta_i) \quad (14)$$

with initial condition $\boldsymbol{x}_f(\eta_i = 0) = \boldsymbol{x}_f(t_i)$, where the vector function $\boldsymbol{g}$ is given by Eqs. (3) and (4). In the integration of the fast dynamics, which is realized by a numerical procedure, the aerodynamic angles are calculated according to $\alpha = \tan^{-1}(w/u)$ and $\beta = \sin^{-1}(v/V)$, where the velocity components in body axes $\mathcal{F}_B$ are obtained as $(u, v, w)^T = \boldsymbol{L}_{BI}\boldsymbol{V}$.

A final comment on α and β: these quantities usually represent an obstacle when dealing with two-timescale problems by one of the approaches that were already proposed in the pertinent literature. This happens because α and β depend on both the slow and the fast states. Sometimes they are just called intermediate time variables.[6] Following the approach presented, no need was felt to introduce an additional intermediate characteristic time, and the angle of attack and the sideslip angle were properly evaluated without numerical difficulty.

III. Results

In all of the applications discussed, the reference vehicle is the F-16 fighter. The mathematical model of the aircraft was completely evaluated following the data in Ref. 9, which apply to the speed range up to a Mach number of 0.6, angle of attack $-20 \le \alpha \le 45$ deg, and sideslip angle $-30 \le \beta \le 30$ deg. The engine thrust, modeled with a first-order lag, is a function of power level, altitude, and Mach number. Considered inputs are control surface deflections δ_A, δ_E, and δ_R and throttle setting δ_T.

Our first results are intended to show how accurately the c.g. trajectory can be calculated by the piecewise helix approximation [Eq. (8)], provided that the dynamic state of the aircraft is correctly known at discrete time intervals. In this case, as in all of the situations that will be discussed later, at the initial time the airplane was in trimmed level flight, at an altitude of 1000 m and at a speed of 100 ms^{-1}.

Figures 2a and 2b show the trajectory of the c.g. of the reference airplane after the aileron angle was changed with the time according to the law presented in Fig. 2c, i.e., $\delta_A(t) = \delta_{Ae} + 0.5\bar{\delta}_A\{1 - \cos[2\pi(t - t_c)/T_{\delta_A}]\}$, where the subscript e stays for equilibrium value, and $\bar{\delta}_A$ and T_{δ_A} are the control amplitude and period, respectively. Two separate inputs were given, at $t_c = 1$ s and $t_c = 11$ s,

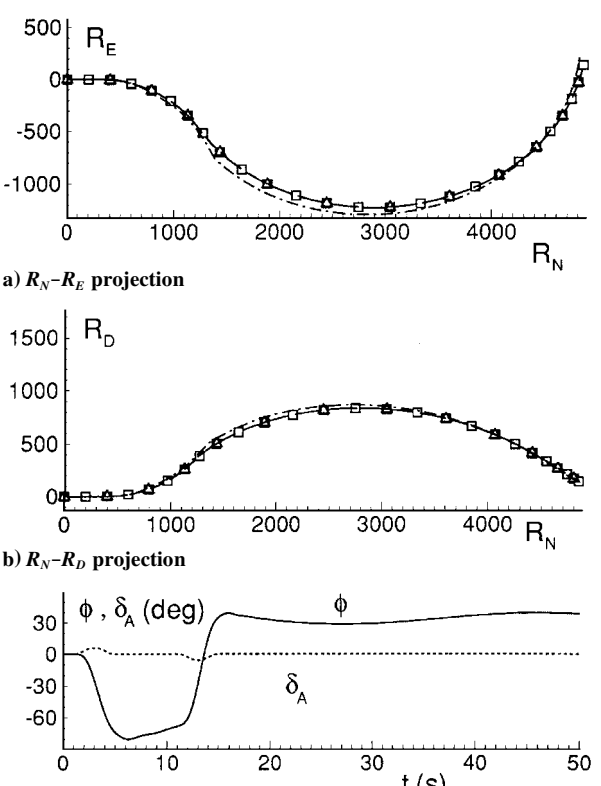

a) R_N–R_E projection

b) R_N–R_D projection

c) Aileron angle δ_A and roll angle ϕ vs t

Fig. 2 Trajectory estimation: □, state sampling at Δt_i = 2 s; △ Δt_i = 4 s; ——, Runge–Kutta code; - - - -, Δt_i = 2 s; and –·–, Δt_i = 4 s.

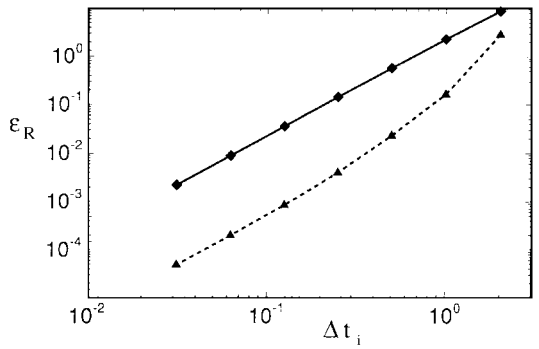

Fig. 3 Error ϵ_R vs Δt_i: ——, second-order expansion and - - - -, third-order expansion.

with $T_{\delta_A} = 4$ s and $\bar{\delta}_A = \pm 6$ deg in the two cases. As a reference, the trajectory and the roll angle ϕ are also shown as they resulted from the application of a fourth-order Runge–Kutta routine with a time step of integration of $\frac{1}{32}$ s (solid lines). The dashed lines show the trajectory as it is analytically estimated at each time interval Δt_i of 2 and 4 s.

At the beginning of each Δt_i, as marked by the symbols □ and △ for $\Delta t_i = 2$ and 4 s, respectively, the initial state with the exception of $\boldsymbol{R}$ was updated by introducing the results of the Runge–Kutta code calculations. It is quite evident that even in the worst case of $\Delta t_i =$ 4 s, the trajectory under the action of the control is satisfactorily predicted over a very long time period. In the circumstance of a real flight, measuring the state of the airplane at discrete times might be sufficient to predict its future location with excellent accuracy, although the errors in the evaluation of the c.g. position progressively sum up.

Let the error in the calculation of the future c.g. position be expressed (in meters) by

$$\epsilon_R = \frac{1}{T}\int_0^T \|\Delta \boldsymbol{R}\|\, \mathrm{d}t$$

where $T = 50$ s is the total time of integration, and $\Delta \boldsymbol{R}$ is the difference between the $\boldsymbol{R}$ value calculated numerically and the value obtained by the expansion for $\boldsymbol{\xi}$. Figure 3 shows ϵ_R as a function of Δt_i over the entire length of about 5800 m of the trajectory in Figs. 2a and 2b. The effect of the order of the series expansion (8) is also shown in Fig. 3, where the solid and dashed lines indicate the second- and third-order approximations of $\boldsymbol{\xi}$, respectively. In the latter case, for Δt_i as high as 2 s, the value of ϵ_R is less than 2 m.

Let us discuss now the application of the approximate solution technique proposed. Figure 4 shows the evolution of some significant quantities during an assigned time variation of the δ_E and δ_A control angles and the influence of the value of Δt_i on the accuracy of the results. For both δ_A and δ_E we chose the same $(1 - \cos)$ law as before, whereas the same values of amplitude and period were maintained as before for δ_A and, to the variation of the elevator angle, the amplitude $\bar{\delta}_E = 2$ deg was given. Again, the solid lines in Fig. 4 are relative to the calculations by the Runge–Kutta code with an integration time step $\Delta\eta_i$ of $\frac{1}{32}$ s. The broken lines correspond to a Δt_i duration of $\frac{1}{2}$ and 1 s, when our procedure is followed, and the series expansion of $\boldsymbol{\xi}$ [Eq. (8)] includes the third-order term. We observe that for $\Delta t_i = 16\Delta\eta_i$ the solid and the broken lines are practically indistinguishable when the evolution of α and q with the time are considered. However, a good accuracy is already obtained for $\Delta t_i = 32\Delta\eta_i$. For p, even $\Delta t_i = 32\Delta\eta_i$ gives excellent results.

Furthermore, θ and ϕ are shown as obtained from the code and from our approach for $\Delta t_i = 32\Delta\eta_i$. The results for these variables are extremely good. Examination of Fig. 4 confirms that the calculation of the angle of attack can be a delicate matter. In fact, for $\Delta t_i = 32\Delta\eta_i$ the error begins to be sizable, although in any case it is less than 10%.

Figure 5 shows how the addition of the third-order term in the power series expansion of $\boldsymbol{\xi}(s)$ increased the accuracy of the results reported so far. The third-order term cited before corresponds to adding a second-order term to the expansion in Eq. (12). The less

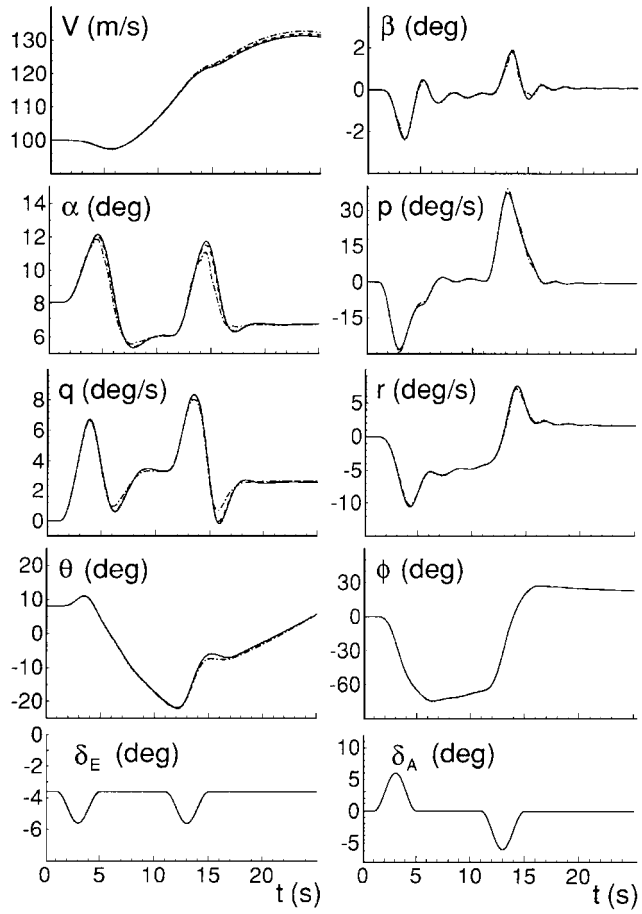

Fig. 4 Time histories of significant variables: ——, fourth-order Runge–Kutta integration; - - - -, $\Delta t_i = 16\Delta\eta_i$; and -·-·-, $\Delta t_i = 32\Delta\eta_i$.

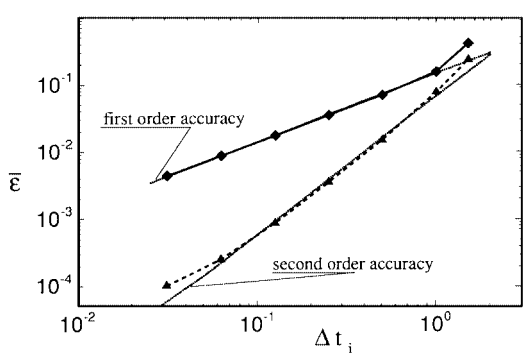

Fig. 5 Error $\bar{\epsilon}$ vs Δt_i: ——, second-order approximation and - - - -, third-order approximation.

accurate, second-order representation of $\boldsymbol{\xi}$ corresponds instead to the prediction of the evolution of the trajectory in the osculating plane at a given instant. The assigned control law on δ_A is as shown in Fig. 2, and, as in the preceding application, only the fast states $\boldsymbol{x}_f$ are numerically integrated. In this case we define the error as

$$\bar{\epsilon} = \frac{1}{N_{\mathrm{st}}}\sum_i \epsilon_i$$

where

$$\epsilon_i = \left\{\left[\int_0^T (x_{i,F} - x_{i,\mathrm{RK}})^2\, \mathrm{d}t\right] \Big/ \left(\int_0^T x_{i,\mathrm{RK}}^2\, \mathrm{d}t\right)\right\}^{\frac{1}{2}}$$

N_{st} is the number of states, and $x_{i,F}$ and $x_{i,\mathrm{RK}}$ indicate the value of the ith state as computed by the present method and by the Runge–Kutta algorithm, respectively. As one can realize from Fig. 5, the

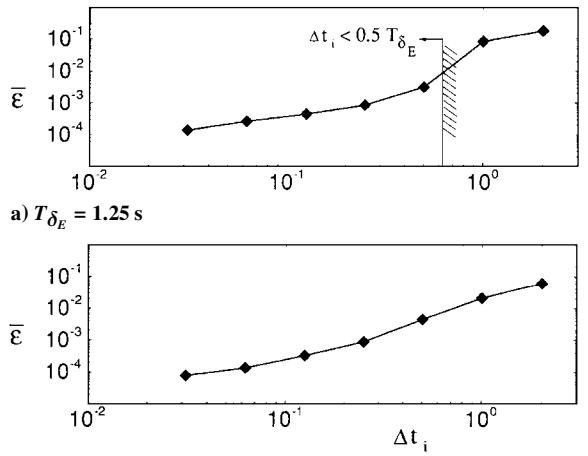

a) $T_{\delta_E} = 1.25$ s

b) $T_{\delta_E} = 10$ s

Fig. 6 Evaluation of the error $\bar{\epsilon}$ for a sinusoidal input on δ_E, $\bar{\epsilon}$ vs Δt_i.

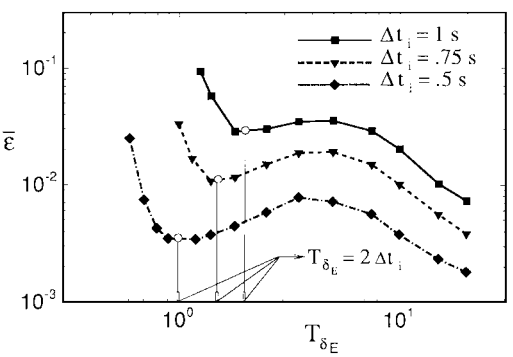

Fig. 7 Evaluation of the error $\bar{\epsilon}$ for a sinusoidal input on δ_E, $\bar{\epsilon}$ vs T_{δ_E} for different values of the sampling interval Δt_i.

improvement in the accuracy increases as the time interval Δt_i decreases and, for the extended series, $\bar{\epsilon}$ can even be of an order of magnitude lower than in the second-order approximation. However, for very small Δt_i, the error in the numerical evaluation of the coefficients of the higher-order terms in the expansion decreases the accuracy of the algorithm.

When the expansion for ξ is halted at the included s^2 term, the error $\bar{\epsilon}$ in the calculation of the c.g. increases with Δt_i, as shown in Fig. 5 by the solid line. In the latter case, the procedure can be effectively called first-order accurate.

Up to this point we have focused our attention on the peculiar but arbitrary maneuver of Fig. 2c, which seemed significant in providing a great deal of information about the capabilities of the method. We want now to be more precise about the influence of the sampling time on the accuracy when the frequency of a prescribed control action is changed. To this purpose we considered the same initial trimmed conditions of the aircraft as before and imposed sine variation of amplitude ± 2 deg to the elevator angle. Figure 6 shows the effects on $\bar{\epsilon}$ of Δt_i for two values of the control period T_{δ_E}, i.e., 1.25 s (Fig. 6a) and 10 s (Fig. 6b). The Nyquist limit related to the sampling frequency is also indicated in Fig. 6a, whereas in Fig. 6b the sampling period is always much smaller than the input signal period. As one would expect, the error reaches its maximum value when the sampling frequency approaches the control frequency and becomes otherwise negligibly small. Last, Fig. 7, for sampling intervals $\Delta t_i = 0.5, 0.75$, and 1.0 s, shows $\bar{\epsilon}$ vs T_{δ_E}. Here the Nyquist critical frequency is interpreted in term of lower limits on the period T_{δ_E}. At frequencies lower than the critical one, the error increases as the input frequency approaches that of the short period mode, the period equal to 4.4 s. Then, as the input period is increased and becomes rather large compared with the sampling interval, the error decreases, as expected, to very low values.

Table 1 Comparison of CPU time: $\Delta\eta_i = \frac{1}{32}$ s, σ_2 second-order expansion, σ_3 third-order expansion

Δt_i, s	σ_2, %	σ_3, %
$\frac{1}{2}$	19.1	17.4
$\frac{1}{4}$	18.5	14.2
$\frac{1}{8}$	17.4	9.9
$\frac{1}{16}$	15.3	2.9

The final results concern the evaluation of the computer time used when the proposed procedure is applied, as compared with fourth-order Runge–Kutta integration of the full set of governing equations. Table 1 reports the percent reduction of CPU time on an IBM RISC/6000 3AT workstation for different values of Δt_i when the series expansion of ξ includes the second (σ_2)- and third (σ_3)-order terms in s. We observe 19 and 17% maximum decreases in CPU time, respectively, with respect to straight Runge–Kutta integration that, in the considered reference simulation, took 18.5 s of CPU time. The noticeable reduction of σ_3 as Δt_i is decreased is due to the time-consuming numerical evaluation of $\ddot{V}$ in the $(k_1')_0$ and $(k_2)_0$ coefficients at the initial time of the interval Δt_i.

IV. Conclusion

The evolution of the dynamical state of an aircraft can be very effectively dealt with when the solution to the motion equations is based on separation of the characteristic timescales and reference is made to the Frenet triad and to the natural coordinates of the c.g. The availability of an analytic solution for the slow dynamics reduces the computational time to that which is necessary for the calculation of a maximum of six fast variables in the most general case.

The accuracy and simplicity of the method make it appealing for a variety of applications, for instance, in guidance and control problems and in the evaluation of maximum performances, where advantage can be taken of both the reduced order of the system and the algebraic expression of the translational states.

Acknowledgments

This work was partially supported by the Italian Ministry for the Universities and Scientific and Technological Research and by the Italian Space Agency.

References

[1] Kepr, B., "Differential Geometry," *Survey of Applicable Mathematics*, edited by K. Rektorys, MIT Press, Cambridge, MA, 1969, pp. 306–317.

[2] Ardema, M. D., "Solution of the Minimum Time-to-Climb Problem by Matched Asymptotic Expansions," *AIAA Journal*, Vol. 14, No. 7, 1976, pp. 843–850.

[3] Calise, A. J., and Markopoulos, N., "Nondimensional Forms for Singular Perturbation Analyses of Aircraft Energy Climbs," *Journal of Guidance, Control, and Dynamics*, Vol. 17, No. 3, 1994, pp. 584–590.

[4] Menon, P. K. A., Badgett, M. E., Walker, R. A., and Duke, E. L., "Nonlinear Flight Test Trajectory Controllers for Aircraft," *Journal of Guidance, Control, and Dynamics*, Vol. 10, No. 1, 1987, pp. 67–72.

[5] Chen, F.-C., and Khalil, H. K., "Two-Time Scale Longitudinal Control of Airplanes Using Singular Perturbation Theory," *Journal of Guidance, Control, and Dynamics*, Vol. 13, No. 6, 1990, pp. 952–960.

[6] Snell, S. A., Enns, D. F., and Garrard, W. L., "Nonlinear Inversion Control for a Supermaneuverable Aircraft," *Journal of Guidance, Control, and Dynamics*, Vol. 15, No. 4, 1992, pp. 976–984.

[7] Stiharu-Alexe, I., and O'Shea, J., "Four-Dimensional Guidance of Atmospheric Vehicles," *Journal of Guidance, Control, and Dynamics*, Vol. 19, No. 1, 1996, pp. 113–122.

[8] Avanzini, G., de Matteis, G., and de Socio, L. M., "Aircraft Equilibrium and Response to Controls in Intrinsic Coordinates," AIAA Paper 97-0323, Jan. 1997.

[9] Stevens, B. L., and Lewis, F. L., *Aircraft Control and Simulation*, Wiley, New York, 1992, pp. 80–89 and 124–127.